

Design and irradiation test of an innovative optical ionization chamber technology

M. Lamotte^a, G. De Izarra^a, C. Jammes^a

^aCEA, DEN DER, Instrumentation Sensors and Dosimetry Laboratory, Cadarache,
F-13108 Saint-Paul-lez-Durance, France.

Abstract

To provide future dependable neutron flux monitoring instrumentation for sodium-cooled fast reactors (SFR) of Generation-IV, French Alternative Energies and Atomic Energy Commission (CEA) is investigating the applicability of an innovative technology based on the optical signal produced within any type of ionization chambers such as fission chambers for instance. A mock-up of that innovative neutron detector was tested on a cold-neutron beamline at the ORPHEE nuclear facility. Experimental results regarding recovery time and detection efficiency showed promising possibilities for neutron instrumentation.

Keywords: fission chambers, radiation-hard detectors, gaseous detectors, gas scintillation

PACS: 29.85.-cAMODIF, 28.50.Dr, 28.41.Rc

1. Introduction

The French Atomic and Alternative Energies Commission (CEA) proposes a new generation of neutron detector for neutron flux monitoring of a sodium-cooled fast reactor [1–5]. This innovative neutron detector is based on the luminescence of rare gases [6]. As in any ionization chambers, heavy ions with high ionization power are generated by a coating layer sensitive to neutrons. The slowing down of heavy ions in rare gas by inelastic collisions generates electrons with a continuous energy distribution ranging from rest up to several keV. The average kinetic energy of

10 primary electrons, about 30 to 50 eV gives them a probability to bring gas atoms
 11 to excited states and produce further secondary electrons until recombinations,
 12 wall or thermal-equilibrium diffusion within the medium [7]. Spontaneous radiative
 13 decay of excited atoms rises emission of photons in the ultraviolet to far-infrared
 14 range [8, 9]. The so-called radiation-induced-absorption (RIA) of silica optical
 15 fibers being minimal in the near-infrared spectrum [10], the transportation of
 16 the generated optical signal in the harsh environment of a nuclear power plant
 17 sounds doable.
 18 Compared to standard ionization chambers and proportional counters, the proposed
 19 optical version of neutron gaseous detectors allow for enhanced on-line self-
 20 diagnosis in terms of working pressure and gas composition [11], increasing the
 21 detector and nuclear reactor dependability thanks to better preventive maintenance
 22 capabilities. In addition, optical ionization chambers are neither affected by
 23 partial discharge effects at high temperature nor electromagnetic noise thanks
 24 to optical signal transmission.
 25 This paper addresses the experimental validation of the CANOE mock-up of
 26 an optical ionization chamber in order to bring a proof of concept of the newly
 27 proposed technology. It starts with the design of the CANOE mock-up. The
 28 measurement setup of the optical signal transmission and detection is then
 29 presented. At last, the experimental results obtained at the ORPHEE nuclear
 30 facility are reported and discussed.

31 **2. Optical ionization chamber mock-ups**

32 An optical fission chamber mock-up, named CANOE (CApteur de Neutrons
 33 à Optique Expérimentale), was designed and built at the French Alternative
 34 Energies and Atomic Energy Commission (CEA). The purpose of this mock-
 35 up is to perform preliminary experimental tests for the sake of technology
 36 development only. This way, at the present phase of our project, it is not
 37 defined to endure the harsh environment of an SFR.
 38 Its main component is an aluminum-alloy-based tube filled with a rare gas

39 such as argon or neon. The neutron-to-heavy-ion conversion can be ensured
 40 by various possible neutron-sensitive materials such as ^6Li , ^{10}B , ^{235}U or ^{239}Pu .
 41 Each one coats the surface of either a 314L-stainless-steel disk of 15 mm diameter
 42 or a 1100 aluminium-alloy tube of 28 mm and about 70 mm long. Fig. 1 shows
 43 a computer-aided cutaway of a CANOE detector, the sensitive component of
 44 which is a boron-coated tube. Tab.1 provides some information on the three
 45 different layers that we employed at the ORPHEE facility (§3.3) such as the
 46 heavy-ion energy deposition rate ΔE .
 47 The cylindrical chamber body is closed by a 10 mm-thick molten-silica window
 48 that is air-tightly sealed with the use of a standard silicon o’ring capable of
 49 standing up to a temperature of 200 °C. That window can be optionally coupled
 50 to a lens assembly in order to focus light on various optical fibers and light pipes
 51 thanks to adapters made on our own using the so-called additive manufacturing
 52 process (3D printing). The gas filling is performed by means of a threaded
 53 titanium nipple pushing a soft-iron ball onto a conical groove.
 54 In addition, a polished pure rhodium disk was placed at the other end, opposite
 55 to the window, so that it helps to reflect photons escaping in the unwanted
 56 direction.

57

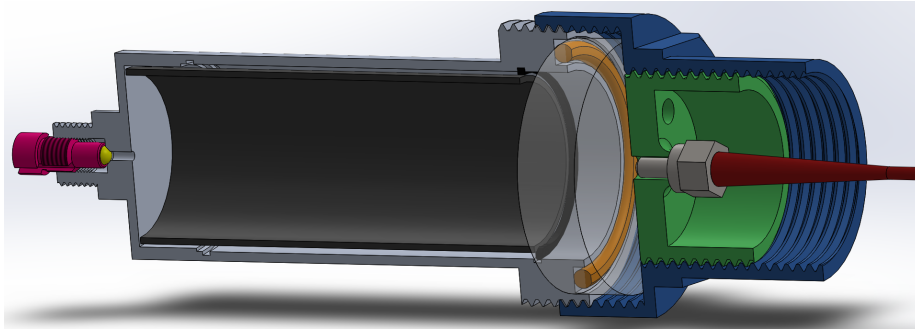
58 **3. Instrumentation and experimental setup**

59 We seized the last opportunity to carry out a partial experimental validation
 60 of the CANOE mock-up at the ORPHEE nuclear facility before its closure at
 61 the end of the year 2019.

62 *3.1. Selection of optical fibers*

63 We had two available types of multi-mode optical fibers. The first one is
 64 a 20 m-long industrial-grade fiber ended by SMA connectors, and featuring a
 65 200 μm -diameter pure silica core and 0.2 Numerical Aperture (NA). The second
 66 fiber type is composed of a 980 μm -diameter core made of PMMA (polymethyl

(a) Computer-aided cutaway



(b) Photography

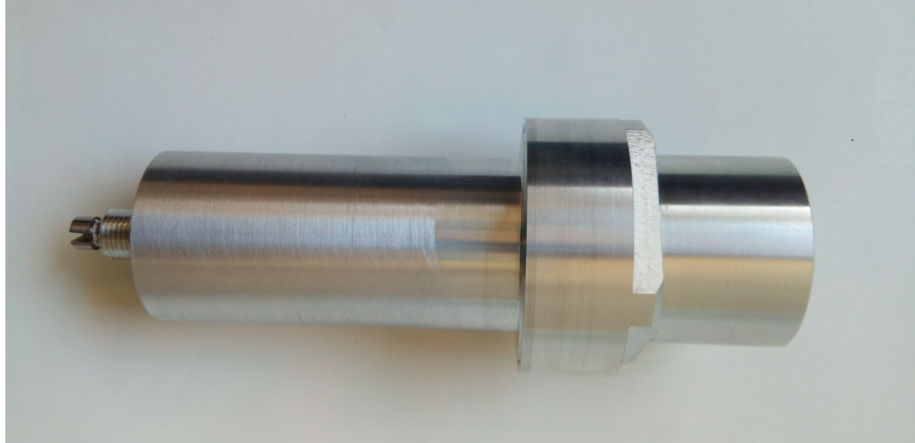


Figure 1: CANOE mock-up. of CANOE. The neutron sensitive layer is enriched a boron carbide, coupled with a 200 μm -diameter core silica fiber, with no use of focusing assembly.

Material	E_0 (MeV)	M (mg)	T (um)	S (cm ²)	σ (b)	ΔE (MeV/s)
²³⁵ U ₃ O ₈	167	0.75	0.51	1.76	1627	1.75E8
¹⁰ B ₄ C	2.31	30	2.0	61.5	10335	1.33E10
²³⁸ PuO ₂	5.5	1.8	0.88	1.76	NA	2.95E9

Table 1: Various sensitive layers for CANOE mock-ups. E_0 (MeV): initial kinetic energy of heavy-ions produced by spontaneous decay or neutron-induced reactions. Surface S: that of ion emission coating of mass M and thickness T. σ : neutron-reaction cross-section at 3.5 meV for fission (²³⁵U) and alpha particle (¹⁰B) production. ΔE : energy deposition rate within the gas for a neutron flux of 8E8 cm⁻².s⁻¹ if 50 % of the ions reach the gas with an energy E_0 . Being an alpha-particle emitter, ²³⁸PuO₂ played the role of a calibration source, the energy deposition rate of which is that of alpha particles.

methacrylate), displaying a NA of 0.5, being able to be cut at wanted length (a 3.5 m-length was actually required). That plastic-made optical fiber, while being unfitted to high neutron fluences and temperatures of an SFR, exhibits neither scintillation nor radiation-induced-absorption in the gamma-particle field met on the cold-neutron beamlines of the ORPHEE facility. Its wider core diameter makes it possible to significantly increase the collected light intensity. As a result, that fiber was selected.

3.2. Multiple light sensor technologies

Two technologies of light sensors were assessed. Fig. 2 presents the experimental setup used for CANOE evaluation: silicon photomultiplier (SiPM) and Geiger-mode avalanche photodiode (APD) were selected for their very good timing performance (recovery time of about a few tens of nanosecond) and high photon-to-electron conversion efficiency (above 15 % at 600 nm). The available large active areas of SiPM allow for light detection from uncollimated light pipes, pulse height analysis and fast recovery time. However, they require a cooling system to reduce dark noise signals.

A Ketek evaluation board embedding a WB-1125 SiPM of 1x1 mm² area was

84 coupled to a low-noise high-frequency monolithic dual stage amplifier consisting
 85 of MAR-3 and MAR-4 chips enabling 12 and 8 dB amplification at 1 GHz,
 86 respectively. The SiPM sensor was polarized with an over-voltage of 3 V, at
 87 room temperature (22 °C) and kept in an aluminium case to prevent electromagnetic
 88 perturbation. The optical fibre was directly coupled through the air to the SiPM
 89 active area.
 90 A Geiger-mode APD was a Peltier-cooled Hamamatsu C13001-01 module offering
 91 on-board temperature regulation, pulse discrimination, signal amplification and
 92 TTL output of 10-ns width. Discrimination threshold is manufacturer-fixed.
 93 The coupling to the APD sensor is ensured by a standard FC optical connector.
 94 Adapters between the bare or SMA-terminated fibers and a CANOE mock-
 95 up were manufactured with a 3D printer. They were then wrapped with an
 96 aluminum ribbon for efficient light-tightness.
 97 Table 2 sums up the most important specification of the employed light sensors
 98 at the ORPHEE facility.

Sensor	DN (cps)	$\tau(ns)$	T(°C)	S (mm ²)	PDE1(%)	PDE2(%)
SiPM WB-1125	65E3	30	22	1.00	32	2.3
APD C13001	17	10	-20	1E-4	20	2.1

Table 2: Main specifications of light sensors used with CANOE mock-ups. DN stands for Dark Noise (without fiber). τ denotes the recovery time, T the substrate temperature and S its surface. PDE 1 and 2 are photon-detection efficiencies at 585 nm and 849 nm, respectively.

99

100 3.3. Setup at ORPHEE

101 As shown in Fig. 3, the CANOE experimental test was performed on the
 102 G3-2 beamline of the ORPHEE facility dedicated to neutron diffusion and
 103 diffraction experiments. The neutron source is provided by a 14 MW highly
 104 enriched uranium-235 pool-type reactor in operation since 1980. The latter is

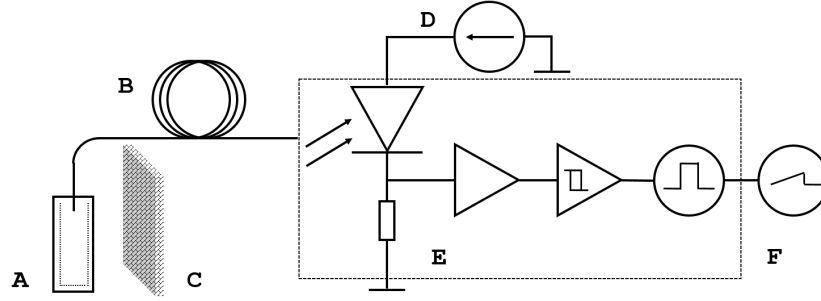


Figure 2: Experimental setup for neutron sensitivity testing of CANOE mock-ups. A: CANOE, B: optical fiber, C: lead shield, D: fixed voltage power supply, E: SiPM or APD signal shaping board, F: oscilloscope .

105 equipped with 9 horizontal tubes, tangential to the core, allowing the use of 20
 106 neutron beams. The common end of those tubes is located in the moderator
 107 near the core, where the flux of thermalized neutrons is maximum. The G3-2
 108 cold neutron beamline of a $25 \times 50 \text{ mm}^2$ section provides a mono-directional flux
 109 as low as $8 \times 10^8 \text{ n.cm}^{-2}.\text{s}^{-1}$ with an average neutron energy of about 3.5 meV.
 110 A boron-coated pneumatic-driven shutter, also referred as to flipper, of about
 111 20 cm high is able to stop the neutron beam within 100 milliseconds. The light
 112 sensors are placed in a lead-shielded casemate [12, 13]. Opening and closing
 113 that casemate is performed manually by pushing a sliding lead door, giving so
 114 an easy access and work-time efficiency.
 115 Because of the low neutron flux available, we had to fill the CANOE mock-ups
 116 with high-purity neon. This way, the emission spectrum was shifted towards
 117 visible wavelengths. Unlike argon, neon at the same pressure enhanced the
 118 detection efficiency of the chosen light sensors as well. For instance, the APD
 119 detection efficiency was significantly improved from 2% at 912 nm with argon
 120 to 32% at 585 nm generated with neon (Fig. 4). Overall, a CANOE mock-
 121 up loaded with 1.8 mg ^{238}Pu , dedicated to calibration as already mentioned,
 122 permitted to obtain up to 4700 cps when filled with neon at 2 atm, whereas
 123 argon at the same pressure led to 72 cps only.

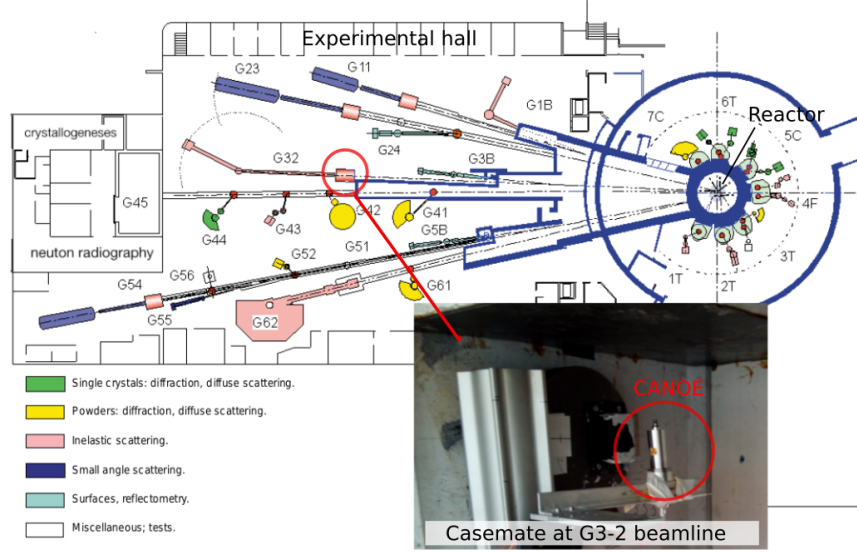


Figure 3: Experimental setup at ORPHEE. The G3-2 cold neutron beamline of a $25 \times 50 \text{ mm}^2$ section provides a mono-directional flux as low as $8 \times 10^8 \text{ n.cm}^{-2}.\text{s}^{-1}$.

124 4. Results and discussion

125 We started to estimate the dark noise signal of the two light sensors, namely
 126 the APD and SiPM ones, by performing an acquisition without CANOE or
 127 fibers. Their active area was covered with a thick fabrics and aluminum foils
 128 while counts were recorded over several minutes to reduce statistical uncertainties.
 129 A count rate ranging between 19 and 25 cps was obtained with APD, whereas
 130 SiPM generated 65,000 cps with a threshold set to 1 PE (photo-electron), the
 131 smallest pulse height achievable, to gather all other pulses of higher intensities
 132 both induced by dark-noise and useful signal.
 133 The unavoidable ambient light at the irradiation location is likely to penetrate
 134 the general-purpose unsheathed optical fibers and come to bias the signal. In
 135 order to limit that bias, the fibers went through a PVC tube. CANOE was then
 136 placed for several minutes into the casemate without neutrons. As the pulse
 137 rate did not increase, the light-tightness of the experimental setup was checked.

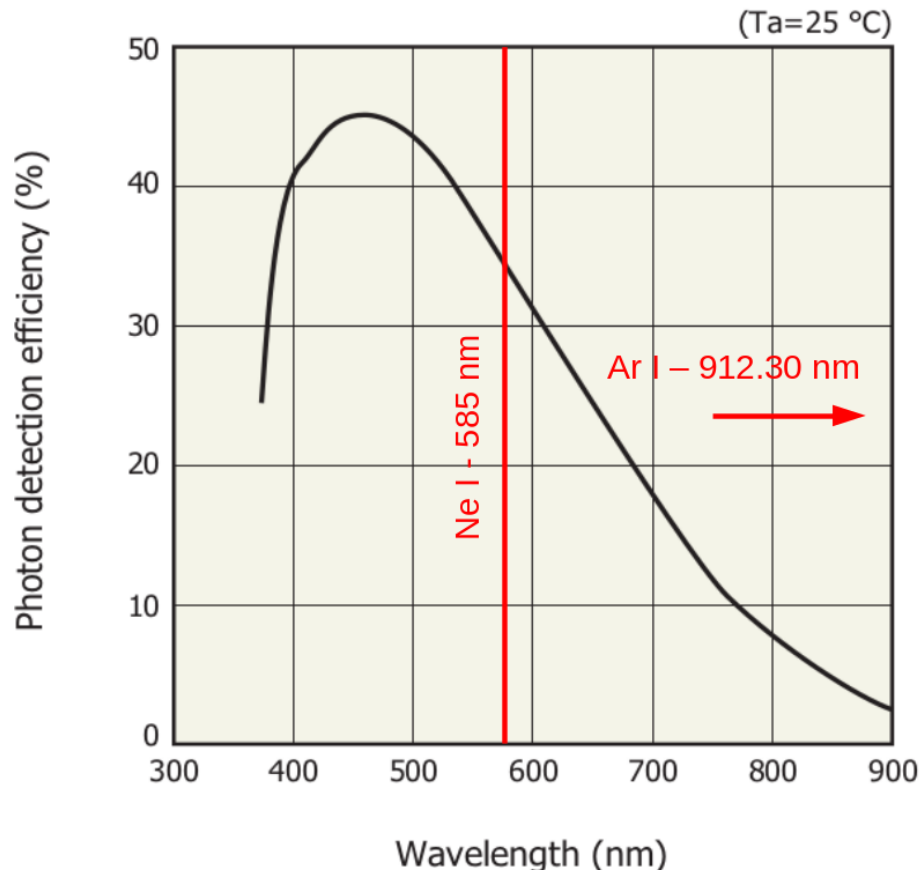


Figure 4: Ratio of detected-to-impacting photons on the APD. Better detection efficiency with neutral neon (Ne I). The APD detection efficiency was significantly improved from 2% at 912 nm with argon to 32% at 585 nm generated with neon.

138 To ensure light being produced in CANOE by heavy-ion interactions in a rare
 139 gas, several irradiations were performed with various configurations shown in
 140 Table 3. It came out that the boron-neon configuration is optimal as expected by
 141 the energy deposition of alpha-particles and lithium ions in the buffer gas under
 142 neutron irradiation. Indeed, when CANOE was filled with high purity neon at
 143 2 atm, opening the neutron beam shutter noticeably increased the count rate
 144 from 25 to 1217 cps with APD. Configurations 3 and 5 clearly shows that the
 145 neutron-induced heavy ions contribute quite totally to the optical signal. Even
 146 though less significant, the count rate of the uranium-neon configuration was
 147 twofold larger under neutron irradiation. Regarding the SiPM sensor, Table 4
 148 shows that even if the dark noise is rather high with 65E3 cps because of the
 149 temperature of the detector, the count rate was doubled during irradiation.
 150 Neutron signal-to-dark-noise ratio is only dependent of the temperature at
 151 constant flux and cooling the SiPM at -25 °C would decrease dark noise to
 152 3E3 cps while the neutron signal would remain as high as 110E3 cps, increasing
 153 signal-to-noise ratio.
 154 The APD signal variation when opening and closing the beam shutter was
 155 also recorded with an Agilent Technologies MSA9104A oscilloscope featuring
 156 a maximum sampling rate of 1 GHz. Due to memory limitation, a recording
 157 time window of 4 s was achievable to carry out such a test. A sampling rate
 158 of 125 MHz was sufficient. Figure 5 shows the experimental output: one can
 159 clearly notice the neutron beam shutter maintained open for 1.8 s.
 160 High-purity uranium fission fragments as source of heavy-ions displayed a similar
 161 trend, even if the overall signal strength was reduced compared to the tubular-
 162 boron excitation source due to smaller sensitive surface.
 163 Finally, the low neutron fluence endured by the optical fibers induced negligible
 164 darkening effects: no difference in signal strength were observed between measurements
 165 over 3 days.

166

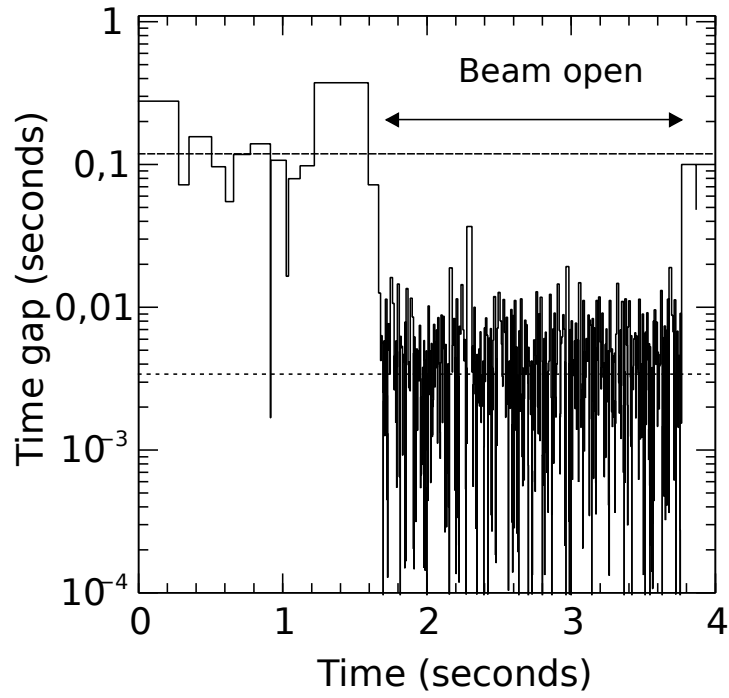


Figure 5: Change in the time gap between logical pulses generated by the APD photon counting module. One can note that the larger the time gap is, the lower the counting rate is. The Geiger-mode APD was coupled to the CANOE mock-up comprising a boron-coated cylinder and 2 atm neon filling gas. The dashed line stands for the average time gap when the beam shutter is closed, whereas the dotted one does for the time gap average when the shutter is open leading to neutron irradiation.

Configuration	Condition	Neutrons	Signal (cps)
1	Boron-air	No	25
2	Boron-air	Yes	102
3	Neon only	Yes	58
4	Boron-neon	No	25
5	Boron-neon	Yes	1217
6	Uranium-neon	No	19
7	Uranium-neon	Yes	66

Table 3: Count rates obtained with APD for various configurations. The sensor was a Hamamatsu C13001-01 cooled Geiger mode APD. Optical fiber made of PMMA and 980 μm diameter was employed unfocused on the sensor and CANOE as well. Configurations 3 and 5 clearly shows that the neutron-induced heavy ions contribute quite totally to the optical signal.

Count rate (cps) at 1 PE (cps)	Neutrons
65E3	No
110E3	Yes

Table 4: Count rates obtained on Ketek WB-1125 SiPM. Optical fibre made of PMMA and 980 μm diameter was employed unfocused on both the light sensor and CANOE. The count rate of the case without neutrons is mostly accounted for by the dark noise effect that could have been significantly reduced by cooling the detector down to -25°C .

167 5. Conclusion

168 The present paper presented preliminary results of optical fission chambers
169 tested at the ORPHEE facility. Two technologies of fast-recovery-time and high-
170 efficiency light detector were evaluated, namely a Geiger-mode cooled Avalanche
171 Photodiode (APD) and Large-area Silicon Photomultiplier (SiPM). Signals from

172 both sensors were strong enough to largely overtake dark counts and follow
 173 operation of a beam shutter of a neutron beamline featuring a weak flux.
 174 Neon as filling gas of the CANOE optical ionization chamber appeared to be
 175 a valuable choice, given its high luminous output in both the visible and near-
 176 infrared spectrum. About 1217 counts per seconds were recorded on a cooled
 177 APD under a $8\text{E}8\text{ n/cm}^2/\text{s}$ neutron flux, with a signal-to-noise ratio of 48.
 178 Even though complementary tests will have to be carried out, the present
 179 irradiation showed that CANOE and its appropriate light sensing technology
 180 was a promising instrumentation for neutron flux monitoring.
 181 Optimization of light collection has to be performed for future application by
 182 means of flexible silica light pipes and optical assembly feeding a cooled light
 183 sensor. One will also have to harden both the chamber components and optical
 184 fiber to stand the harsh environment of a sodium-cooled fast reactor.

185 Acknowledgments

186 The authors are very thankful to the ORPHEE staff and more particularly
 187 to A. Menelle, F. Gibert for their general support and valuable advices, making
 188 the experiment possible.

189 References

- 190 [1] P. Filliatre, C. Jammes, B. Geslot, Stopping power of fission fragments of
 191 Cf-252 in argon: A comparison between experiments and simulation with
 192 the SRIM code, Nucl. Instrum. Methods Phys. Res. A 618 (1-3) (2010)
 193 294–297. doi:10.1016/j.nima.2010.02.270.
- 194 [2] C. Jammes, P. Filliatre, B. Geslot, T. Domenech, S. Normand, Assessment
 195 of the High Temperature Fission Chamber Technology for the French Fast
 196 Reactor Program, IEEE TRANSACTIONS ON NUCLEAR SCIENCE
 197 59 (4, 2) (2012) 1351–1359, 2nd International Conference on Advancements
 198 in Nuclear Instrumentation, Measurement Methods and their Applications,
 199 Ghent, BELGIUM, JUN 06-09, 2011. doi:10.1109/TNS.2012.2205161.

200 [3] C. Jammes, N. Chapoutier, P. Filliatre, J. P. Jeannot, F. Jadot, D. Verrier,
201 A. C. Scholer, B. Bernardin, Neutron flux monitoring system of the
202 French GEN-IV SFR: Assessment of diverse solutions for in-vessel detector
203 installation, NUCLEAR ENGINEERING AND DESIGN 270 (2014) 273–
204 282. doi:10.1016/j.nucengdes.2013.12.057.

205 [4] Z. S. Elter, C. Jammes, I. Pazsit, L. Pal, P. Filliatre, Performance
206 investigation of the pulse and Campbell modes of a fission chamber
207 using a Poisson pulse train simulation code, Nucl. Instrum. Methods Phys.
208 Res. A 774 (2015) 60–67. doi:10.1016/j.nima.2014.11.065.

209 [5] G. Galli, H. Hamrita, C. Jammes, M. J. Kirkpatrick, E. Odic, P. Dessante,
210 P. Molinie, B. Cantonnet, J. C. Nappe, Characterization and Localization
211 of Partial-Discharge-Induced Pulses in Fission Chambers Designed for
212 Sodium-Cooled Fast Reactors, IEEE Trans. Nucl. Sci. 65 (9, 1) (2018)
213 2412–2420. doi:10.1109/TNS.2018.2861566.

214 [6] M. Lamotte, G. De Izarra, C. Jammes, Heavy-ions induced scintillation
215 experiments, J. Instrum. 14 (09) (2019) C09024.

216 [7] L. Koch, Étude de la fluorescence des gaz rares excités par des particules
217 nucléaires. Utilisation pour la détection des rayonnements nucléaires.,
218 Ph.D. thesis, Université de Paris (1959).

219 [8] W. R. Bennett, Optical spectra excited in high pressure noble gases by
220 alpha impact, Ann. Phys. 18 (2) (1962) 367 – 420.

221 [9] A. A Abramov, V. V Gorbunov, S. P Melnikov, A. Kh Mukhamatullin,
222 A. Pikulev, A. V Sinitsyn, A. A Sinyanskii, V. M Tsvetkov, Luminescence
223 of nuclear-induced rare-gas plasmas in near infrared spectral range, Vol.
224 6263, 2005. doi:10.1117/12.677457.

225 [10] G. Cheymol, H. Long, J.-F. Villard, B. Brichard, High level gamma and
226 neutron irradiation of silica optical fibers in CEA OSIRIS nuclear reactor,
227 IEEE Trans. Nucl. Sci. 55 (4) (2008) 2252–2258.

- 228 [11] M. Lamotte, G. de Izarra, C. Jammes, Development and first use of an
229 experimental device for fission-induced spectrometry applied to neutron
230 flux monitoring, Nucl. Instrum. Methods Phys. Res. A (2019) 163236.
- 231 [12] V. Méot, O. Roig, B. Rossé, P. Morel, J.-M. Daugas, D. Doré,
232 A. Letourneau, A. Menelle, Direct measurement of the inelastic neutron
233 acceleration by 177mlu, in: EPJ Web Conf., Vol. 2, EDP Sciences, 2010,
234 p. 05004.
- 235 [13] E. Simon, P. Guimbal, Performance assessment of imaging plates for the
236 JHR transfer Neutron Imaging System, in: EPJ Web Conf., Vol. 170, EDP
237 Sciences, 2018, p. 04021.